Bioorganic Chemistry 86 (2019) 126–136

Contents lists available at ScienceDirect

Bioorganic Chemistry

journal homepage: www.elsevier.com/locate/bioorg

Synthesis of 5-enamine-4-thiazolidinone derivatives with trypanocidal and anticancer activity

Serhii Holota[a,f], Anna Kryshchyshyn[a], Halyna Derkach[b], Yaroslava Trufin[a], Inna Demchuk[a], Andrzej Gzella[c], Philippe Grellier[d], Roman Lesyk[a,e,*]

[a] Department of Pharmaceutical, Organic and Bioorganic Chemistry, Danylo Halytsky Lviv National Medical University, 69 Pekarska, Lviv 79010, Ukraine
[b] Department of Chemistry, Ivano-Frankivsk National Medical University, 2 Halytska, Ivano-Frankivsk 76018, Ukraine
[c] Department of Organic Chemistry, Poznan University of Medical Sciences, Grunwaldzka 6, 60-780 Poznan, Poland
[d] National Museum of Natural History, UMR 7245 CNRS-MNHN, Team APE, CP 52, 57 Rue Cuvier, Paris 75005, France
[e] Department of Public Health, Dietetics and Lifestyle Disorders, Faculty of Medicine, University of Information Technology and Management in Rzeszow, Sucharskiego 2, 35-225 Rzeszow, Poland
[f] Department of Organic Chemistry and Pharmacy, Lesya Ukrainka Eastern European National University, Volya Avenue 13, 43025 Lutsk, Ukraine

ARTICLE INFO

Keywords:
5-ene-4-thiazolidinones
Antitrypanosomal activity
Anticancer activity
X-ray

ABSTRACT

A series of novel 2-(5-aminomethylene-4-oxo-2-thioxothiazolidin-3-yl)-3-phenylpropionic acid ethyl esters has been synthesized. Target compounds were evaluated for their trypanocidal activity towards *Trypanosoma brucei brucei* and *Trypanosoma brucei gambiense*. Several hit-compounds (**8**, **10**, **12**) inhibited growth of the parasites at sub-micromolar concentrations (IC_{50} 0.027–1.936 μM) and showed significant selectivity indices (SI = 108–1396.2) being non-toxic towards the human primary fibroblasts. The screening of anticancer activity *in vitro* within NCI DTP protocol allowed to identify active 2-(5-{[5-(2,4-dichlorobenzyl)-thiazol-2-ylamino]-methylene}-4-oxo-2-thioxothiazolidin-3-yl)-3-phenylpropionic acid ethyl ester **14** that demonstrated inhibition against all 59 human tumor cell lines with the average GI_{50} value of 2.57 μM. It was established that the activity type (antitrypanosomal or anticancer) as well as its level depends on the character of enamine fragment in the C5 position of thiazolidinone core.

1. Introduction

Human African Trypanosomiasis (sleeping sickness) belongs to the neglected parasitic diseases and is caused by protozoa *Trypanosoma brucei gambiense (Tbg)* and *Trypanosoma brucei rhodesiense* (Tbr) transmitted by the tsetse fly. Great advances have been made in HAT control and as a result the number of new cases of sleeping sickness had dropped to less than 3000 in 2015 [1], though near 60 million of people in Sub-Saharan Africa remain at risk for infection. Untreated the disease is usually fatal. There was no new drug approved since 90th, when eflornithine, initially developed as anticancer drug, was registered for the second stage HAT treatment [2]. Rather toxic arsenic derivative melarsoprol has been used as a second line treatment for the late-stage *Tbg* sleeping sickness until now. And it is the only drug available for the late-stage *Tbr* infection treatment [3]. The combination therapy with eflornithine and nifurtimox (NECT), registered for Chagas disease, has appeared as an alternative to eflornithine monotherapy. Though, it has not reduced the price of the treatment. One more problem associated with mentioned drugs is their injectable route of administration. Thus, there is a need in new effective and non-toxic drugs for the HAT treatment. Our study of new potential trypanocidals covers the investigation of 4-thiazolidinone derivatives as potent antitrypanosomals (see Scheme 1).

4-Thiazolidinone derivatives are known for a wide range of biological activity. Anticancer, anti-inflammatory, antituberculosis as well as antimicrobial effects are the most studied for this class of drug-like molecules [4–9]. Recently, 4-thiazolidinone and thiazole derivatives have been investigated as potent trypanocidal compounds [10–12], not the least due to their evident antitumor potential when the so-called “repurposing strategy” is applied [13–16]. In some way, they are treated as cyclic analogs of thioureas/thiosemicarbazides [17–19] – a thoroughly studied class of antitrypanosomal agents [20]. Arguments approving the search for antitrypanosomals among 5-aminomethylene-4-thiazolidinone derivatives were the next: (i) the established inhibitory

* Corresponding author at: Department of Pharmaceutical, Organic and Bioorganic Chemistry, Danylo Halytsky Lviv National Medical University, 69 Pekarska, Lviv 79010, Ukraine.
E-mail address: dr_r_lesyk@org.lviv.net (R. Lesyk).

https://doi.org/10.1016/j.bioorg.2019.01.045
Received 19 November 2018; Received in revised form 20 December 2018; Accepted 20 January 2019
Available online 22 January 2019

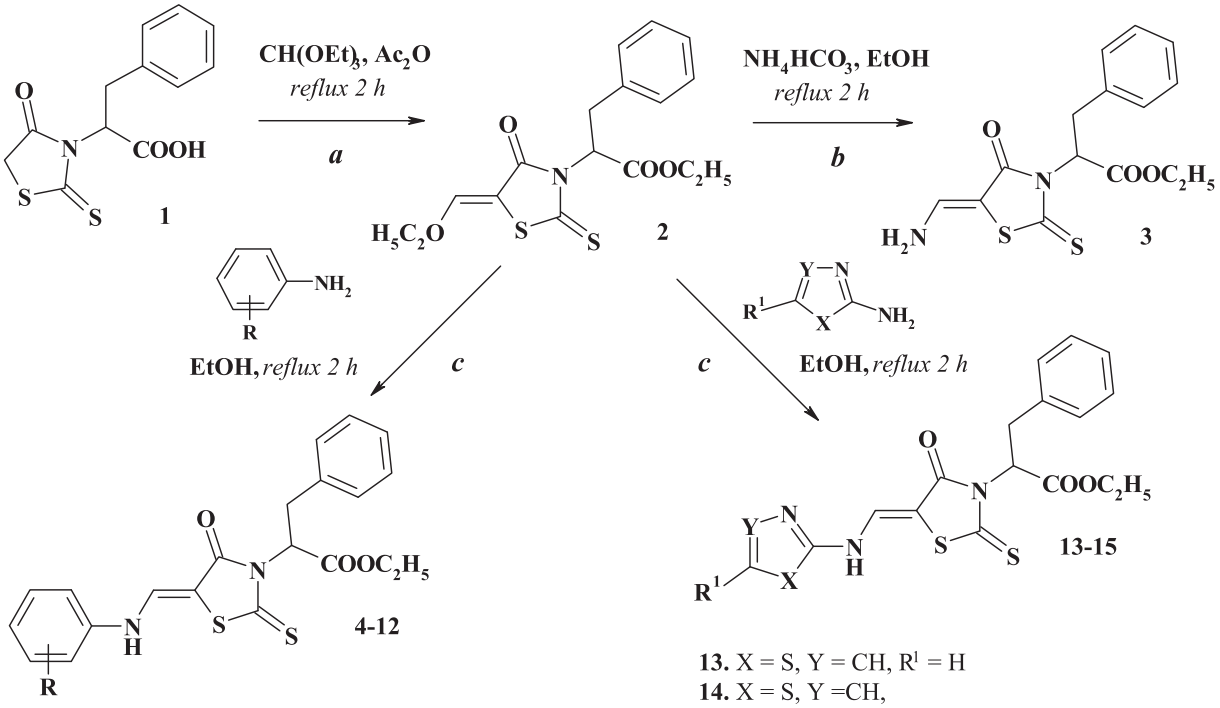

4. R = H
5. R = 4-Cl
6. R = 4-F
7. R = 2-NO_2-4-Cl
8. 2-MeO-5-Cl
9. 4-SO_2NH_2
10. R = 2-Me-5-(morpholine-4-sulfonyl)
11. R = 4-SO_2SEt
12. R = 4-COOEt

13. X = S, Y = CH, R^1 = H
14. X = S, Y =CH, R^1 = 2,4-Cl_2-$C_6H_3CH_2$
15. X = NH, Y = N, R^1 = H

Scheme 1. Synthesis of 2-(5-aminomethylene-4-oxo-2-thioxothiazolidin-3-yl)-3-phenylpropionic acid ethyl ester derivatives **3–15**. Reagents and conditions: (a) **1** (10 mmol), $CH(OEt)_3$ (12 mmol), Ac_2O (10 mL), 2 h, reflux, 72%; (b) **2** (10 mmol), NH_4HCO_3 (10 mmol), EtOH (20 mL), reflux, 2 h, 54%; (c) **2** (10 mmol), amine (10 mL), EtOH (20 mL), reflux, 2 h, 53–71%.

activity of 5-benzylidenerhodanine-3-acetic acid derivatives against *T. brucei* dolicholphosphate mannose synthase and glycosylphosphatidylinositol anchor synthesis [21]; (ii) the established trypanocidal activity of some 5-(3-naphthalen-2-yl-5-aryl-4,5-dihydropyrazol-1-yl)-thiazolidine-2,4-diones [22]; (iii) the investigated trypanocidal activity of pyrazoline-thiazolidinone conjugates and proved activity increasing with the introduction of alkyl or aryl substituents in the N3 position of thiazolidinone core [23]. Although, in recent high-throughput screening (HTS) campaigns 5-ene-thiazolidinones are treated as PAINS [24] as well as possible Michael acceptors, herein we would like to stress that classical pharmacological screening differs from the HTS. The molecular hybridization approach was used for the direct synthesis of the limited series of 5-aminomethylene-4-thiazolidinones to study them in *in vitro* assays towards the cultures of parasites. Moreover, it should be noted that there are a number of approved efficient drugs – 4-thiazolidinediones [25] and the behavior of Michael acceptors in the human organism is not so unambiguously investigated [4,5] till now. We have also decided to combine the thiazolidine ring and phenylalanine fragments in the molecules in order to mimic the amide bond of peptides. Substances belonging to peptidomimetics have been also studied as potent antitrypanosomals [26,27].

2. Results and discussion

2.1. Chemistry

Target compounds were synthesized using known synthetic protocol [9,28,29] including stage of 2-(4-oxo-2-thioxothiazolidin-3-yl)-3-phenylpropionic acid **1** formation [30]. Further condensation with triethyl orthoformate yielded 5-ethoxy-4-thiazolidinone **2**. Interesting was the simultaneous esterification of the carboxylic group that resulted in the ester formation. 5-Ethoxy-4-thiazolidinone **2** was converted into appropriate enamines **3–15** in the reactions with ammonium hydrogen carbonate, different primary aromatic and heterocyclic amines in ethanol medium.

Structures of the synthesized compounds were confirmed by the elemental analysis and spectroscopic data (^{1}H NMR, ^{13}C NMR and LCMS). It is known that the primary and secondary enamines are characterized by enamine-imine tautomerism [31]. Therefore, spectroscopic studies revealed characteristic duplication of signals in ^{1}H and ^{13}C NMR spectra or the formation of multiplets due to the overlapping of signals, observed for some synthesized compounds. This may be probably linked to the co-existence of two different tautomeric forms. On the basis of the ^{1}H NMR spectra and LCMS, the ratio of tautomers varies from 1:1 for the derivatives with *ortho*-methyl- and methoxyphenylamino group (**8**, **10**) to 9:1 for other compounds. In ^{1}H NMR spectra the characteristic aminomethylene group (NH = CH) of

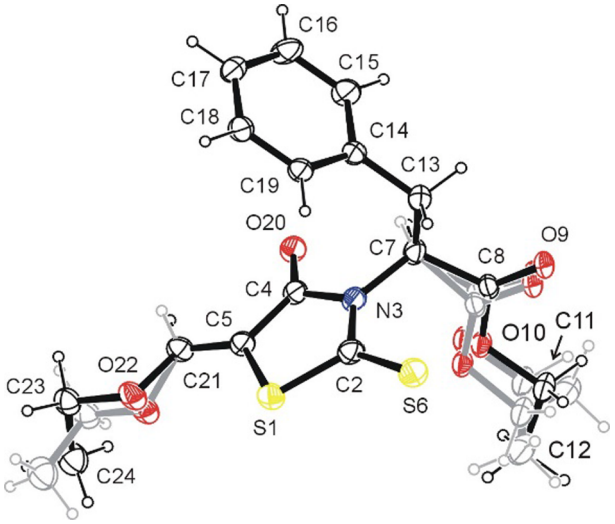

Fig. 1. ORTEP view of **2** showing the atomic labelling scheme. Non-H atoms are drawn as 30% probability displacement ellipsoids and H atoms are drawn as spheres of an arbitrary radius. The disordered parts of the molecules are colored grey, as distinct from the major component shown in black.

synthesized compounds **4–15** showed two doublets ($J \sim 12.0$ Hz) or broad singlets at $\delta \sim 7.91$–8.65 and $\delta \sim 10.20$–12.20 ppm.

Structural features of the starting compound **2** as well as the key 5-enamine derivatives **3** and **12** were confirmed by X-ray crystallographic analysis.

A structure of the compound **2** obtained in an X-ray analysis is presented in Fig. 1. According to the study, the ethoxymethylene and ethoxycarbonyl groups in the crystal are disordered. The first one may be spatially oriented in two ways (orientation A and B). Torsion angles C5–C21–O22–C23 found {with atoms O22A, C23A: −176.6(2)°; with atoms O22B, C23B: −167.8(11)°} and C21–O22–C23–C24 {with atoms O22A, C23A, C24A: 94.4(3)°; with atoms O22B, C23B, C24B: −161.8(17)°} show that bonds C5–C21 and O22A(B)–C23A(B) take an antiperiplanar conformation whereas bonds C21–O22A(B) and C23A(B)–C24A(B) an intermediate conformation between synclinal and anticlinal ones and an antiperiplanar conformation, respectively. Atoms O22, C23 and C24 in location A have got a site occupancy factor of 0.8495 whereas in location B – 0.1505. The latter group has got three different spatial locations in a crystal. These are determined in torsion angles C7–C8–O10–C11 and C8–O10–C11–C12. In atoms C8, O10, C11, C12 in orientation A, the angles are −178.6(3) and 176.8(5)°, respectively. It means that bonds C7–C8A and O10A–C11A as well as C8A–O10A and C11A–C12A take an antiperiplanar conformation. In case of the same atoms in orientations B and C, torsion angles are −175.7(7) and 98.2(11)°, and −176.3(9) and −83.6(13)° respectively. It means that bonds in pairs C7–C8/O10–C11 and C8–O10/C11–12 within an ethoxycarbonyl group in orientations B and C take an antiperiplanar conformation and an intermediate conformation between synclinal and anticlinal ones (+sc/+ac; −sc/–ac). Various signs +/– mean that an atom C12 deflects in opposite directions from a flat system of the other atoms in the group. Site occupancy factor for the group of atoms C8, O10, C11, C12 in location A is 0.5357, in location B 0.2348, in location C 0.2303. A phenyl system present in the molecule, which is a part of an 1-ethoxy-1-oxo-3-phenylpropan-2-yl residue, forms a dihedral angle of 50.91(6)° with a thiazolidine system. A spatial orientation of the phenyl system in the molecule is also determined by torsion angles C2–N3–C7–C13 and N3–C7–C13–C14 of −72.5(2) i −58.4(2)° respectively.

Based on X-ray diffraction study it was established that the compound **3** crystallized in the centro-symmetric space group $P2_1/c$ with two independent molecules A and B in the asymmetric unit, being a pair of *R* and *S* enantiomers (Fig. 2). The chiral center in the molecules is in C7 position. Independent molecules A and B are mirrored for each other. In a molecule B of an absolute configuration *R*, a spatial orientation of an ethoxycarbonyl group, which is a part of 1-ethoxy-1-oxo-3-phenylpropan-2-yl residue, is determined by torsion angles C2B–N3B–C7B–C8B [118.0(3)°], N3B–C7B–C8B–O9B [152.1(3)°] and C8B–O10B–C11B–C12B [−83.2(5)°]. According to their values, bonds C2B–N3B and C7B–C8B take an anticlinal conformation, bonds N3B–C7B and C8B–O9B an intermediate conformation between anticlinal and antiperiplanar ones, whereas bonds C8B–O10B and C11B–C12B an intermediate conformation between a synclinal and anticlinal ones. A spatial orientation of a phenyl group in the mentioned molecule's fragment is determined by torsion angles C2B–N3B–C7B–C13B [−115.3(3)°] and N3B–C7B–C13B–C14B [50.1(3)°], and by dihedral angle between 2-thioxo-4-thiazolidinone and phenyl systems. According to the values of the torsion angles, bonds C2B–N3B and C7B–C13B take an anticlinal conformation to each other, whereas bonds N3B–C7B and C13B–C14B a synclinal one. A dihedral angle between the flat ring systems is 52.43(8)°.

Having compared the geometry of molecules in the compound **3** (molecule A) and the compound **2** discussed above, both of which have an absolute configuration *S*, it was observed that in these molecules ethoxycarbonyl and benzyl moieties change their places as a result of a rotation of 1-ethoxy-1-oxo-3-phenylpropan-2-yl residue around a bond N3–C7 by ca. 180°. It was proved by torsion angles C2–N3–C7–H7(A/B/C) (compound **2**: −169/−178/−170°, compound **3**, molecule A: −2°). Three different values of the discussed torsion angle for a molecule in a compound **2** are connected with a disorder of an ethoxycarbonyl group in a crystal. The observed interatomic C5–C21 distances in molecules A

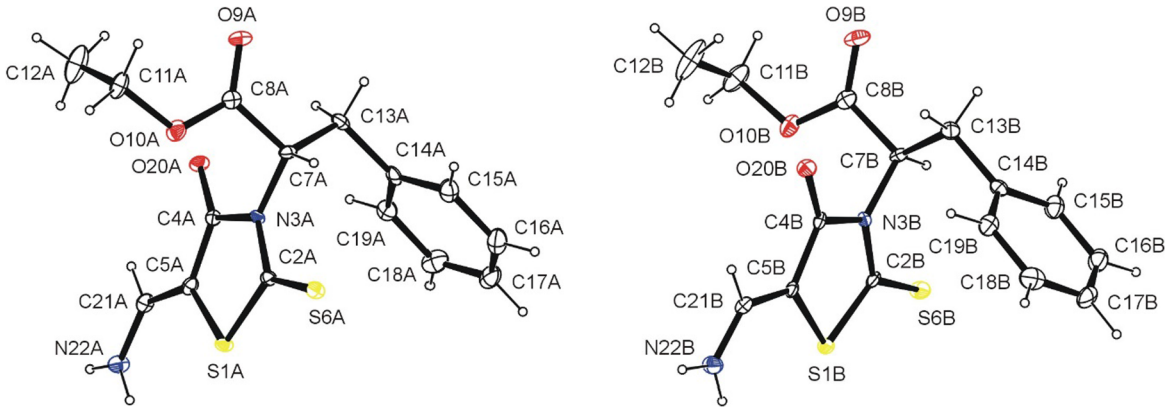

Fig. 2. ORTEP view of two symmetry-independent molecules (A and B) of **3** showing displacement ellipsoids at the 30% probability level. H atoms are shown as spheres of arbitrary radii.

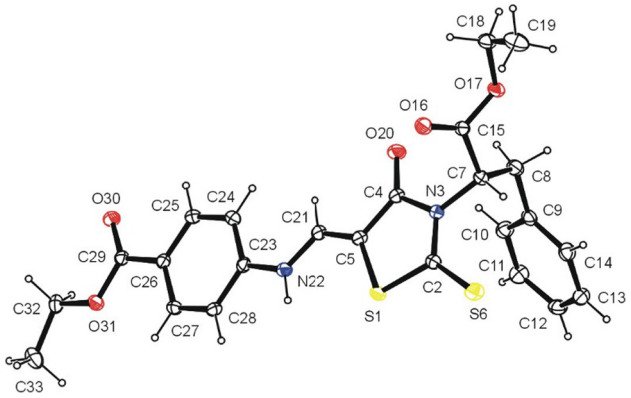

Fig. 3. ORTEP view of **12** showing the atomic labelling scheme. Non-H atoms are drawn as 30% probability displacement ellipsoids and H atoms are drawn as spheres of an arbitrary radius.

and B {1.363(4) and 1.361(4) Å, respectively} confirm the presence of a double bond between these atoms.

A structure of the compound **12** obtained in an X-ray analysis was presented in Fig. 3. According to the research, the compound is a stereoisomer *Z*. An obtained torsion angle S1–C5–C21–N22 is −0.5(4)°. In a molecule, a phenyl system (C9–C14), which is a part of a 1-ethoxy-1-oxo-3-phenylpropan-2-yl residue, forms a dihedral angle of 54.80(8)° with a heterocyclic 2-sulfanylidene-4-thiazolidinone system. Spatial orientation of a phenyl ring of the molecule is also determined by torsion angles C2–N3–C7–C8 and N3–C7–C8–C9 of 110.8(2) and −48.7(3)°, respectively. Whereas geometry of an ethoxycarbonyl group (C15,O16,O17,C18,C19) is present in 1-ethoxy-1-oxo-3-phenylpropan-2-yl residue, is determined by torsion angles C2–N3–C7–C15, N3–C7–C15–C17 and C15–O17–C18–C19 of −120.3(2), −155.8(2) and 92.0(3)° respectively. Value of the last torsion angle suggests significant deflection of an atom C19 from a flat system (r.m.s. = 0.0119 Å) composed of other atoms in this group. It was discovered that this atom deflects by 1.404(5) Å. It is important that the spatial configuration of a 1-ethoxy-1-oxo-3-phenylpropan-2-yl residue in a molecule of a compound **12** with an absolute configuration *S* is similar to a spatial orientation of the same group in a molecule with configuration *S* in the compound **3**. A torsion angle C2–N3–C7–H7 is ca. −5°.

A remaining fragment of the molecule including 5-{[(4-ethoxycarbonylphenyl)-amino]-methylene}-2-thioxo-4-thiazolidinone moiety is approximately flat. It means that an ethoxycarbonyl (C29, O30, O31, C32, C33) group, which is a part of this fragment, is approximately flat (r.m.s. = 0.0141 Å), unlike an ethoxycarbonyl group of the 1-ethoxy -1-oxo-3-phenylpropan-2-yl residue.

According to the research, a nitrogen atom N22 present in the molecule is of amine character. Location of a hydrogen atom was determined on the basis of Fourier map and was refined freely. The confirmation of its presence in the N22 position are: hydrogen bonds N22–H22···O30^{i} {N22–H22 0.85(3) Å, H22···O30 2.00(3) Å, N22···O30 2.840(3) Å, N22–H22···O30^{i}: 166 (3) °; (i) *x*, 0.5–*y*, 0.5 + *z*}, with the amino group (N22–H22) as the donor and a carbonyl oxygen atom (O30) as a proton's acceptor (Fig. 4).

2.2. Antitrypanosomal activity

The antitrypanosomal activity of the novel compounds **3–15** was studied in *in vitro* assay towards *Trypanosome brucei brucei (Tbb)* and *Trypanosoma brucei gambiense (Tbg)*. The IC_{50} values were calculated based on at least three independent experiments. Cytotoxicities against myoblast-derived cell line (L-6) were determined to calculate the selectivity indices SI (the ratios of cytotoxic CC_{50} values to antitrypanosomal IC_{50} values).

In general, 2-(5-aminomethylene-4-oxo-2-thioxothiazolidin-3-yl)-3-phenylpropionic acid ethyl esters inhibited the parasites growth at micro- and submicromolar concentrations (Table 1). The influence of different aryl/heteryl substituents in the C5 of thiazolidinone ring as well as the importance of the molecular modification of arylidene fragment were studied. Introduction of the thiazole and triazole rings (compounds **13**, **14**, **15**) didn't significantly contribute to improving the potency and considerably increased the toxicity levels. On the other hand, the efficacy of 2-(5-aminomethylene-4-oxo-2-thioxothiazolidin-3-yl)-3-phenylpropionic acid ethyl esters with different phenyl fragments (**4–10**, **12**) against the parasites (IC_{50}s 0.091–3.916 μM for *Tbb* and 0.027–1.936 μM for *Tbg*) was notably higher than such of the unsubstituted 5-aminomethylene derivative **3** (IC_{50}s 37.551 μM for *Tbb* and 11.592 μM for *Tbg*). Based on the established levels of trypanocidal activity towards *Tbg* and the toxicity towards human fibroblasts, the most active compounds were **8**, **10** and **12** with the SI within 158–1396.2. For comparison, the selectivity indices for reference drugs Pentamidine and Nifurtimox were 5396.9 and 14.0 respectively. The same trend was observed for active compounds in the anti-*Tbb* assays: SI = 108–409.4 in comparison with the selectivity index 27.2 for Nifurtimox and 5793.9 for Pentamidine. Among tested compounds, 5-(4-ethoxycarbonylphenyl)aminomethylene derivative **12** showed the highest trypanocidal activity with IC_{50} values of 0.091 μM for *Tbb* and 0.027 μM for *Tbg* respectively. In addition this compound had selectivity index 15- (*Tbb*) and 100-times (*Tbg*) higher than Nifurtimox.

SAR emerged from these data revealed that a combination of thiazolidinone ring with arylaminomethylene fragment in C5 position and phenylpropionic acid ester moiety in the N3 position significantly contribute to improving the antitrypanosomal potency of this family of small organic molecules. Moreover, the impact of phenylpropionic acid ester moiety on trypanocidal activity of the similar *N*-non-substituted 5-phenylaminomethylene-rhodanines was proved by their significantly higher IC_{50} values [32]. The obtained results revealed that substituent variation in the arylaminomethylene had considerably influenced the antitrypanosomal activity. Thus, for 5-arylenamine derivatives the activity increases in the row of the following substituents: 4-SO_2SEt < 4-SO_2NH_2 < H < 2-MeO-5-Cl < 4-F < 2-NO_2-4-Cl < 4-Cl or 2-Me-5-(morpholine-4-sulfonyl) < 4-COOEt.

2.3. In vitro evaluation of the anticancer activity

Taking into account the results of previous studies of thiazolidinones [28,29] and following the concept of «multifunctional drugs» [33–35], a series of 5-enamine-4-thiazolidinones were studied for their anticancer activity. Thus, compounds **3**, **4**, **6**, **8**, **11**, **14** and **15** were selected by National Cancer Insitute (NCI, Bethesda, USA) Developmental Therapeutic Porgram (DTP) and tested at one dose assay (10^{-5} M) toward a panel of approximately sixty cancer cell lines representing different types of cancer (leukemia, melanoma, lung, colon, CNS, ovarian, renal, prostate and breast cancers). Primary anticancer assays were performed according to the NCI protocol as described elsewhere [36–39]. The compounds were added at a single concentration and the cell cultures were incubated for 48 h. The end point determinations were made with a protein binding dye, sulforhodamine B (SRB). The results for each compound are reported as the percent growth (GP%) of treated cells compared to untreated control cells (Table 1). The range of percent growth shows the lowest and the highest percent growth found among the different cancer cell lines. The highest growth inhibition rates were observed for the derivative **14**, while unsubstituted amino group in **3**, aniline fragments in **4**, **6**, **8**, **11** and triazole cycle in **15** didn't contribute to the antiproliferative activity (see Table 2).

Compound **14** was selected for the in-depth screening at a range of concentrations towards 59 cell lines. The percentage of growth was evaluated spectrophotometrically versus controls not treated with test agents after 48-h exposure and using SRB protein assay to estimate cell viability or growth. Three antitumor activity dose-response parameters

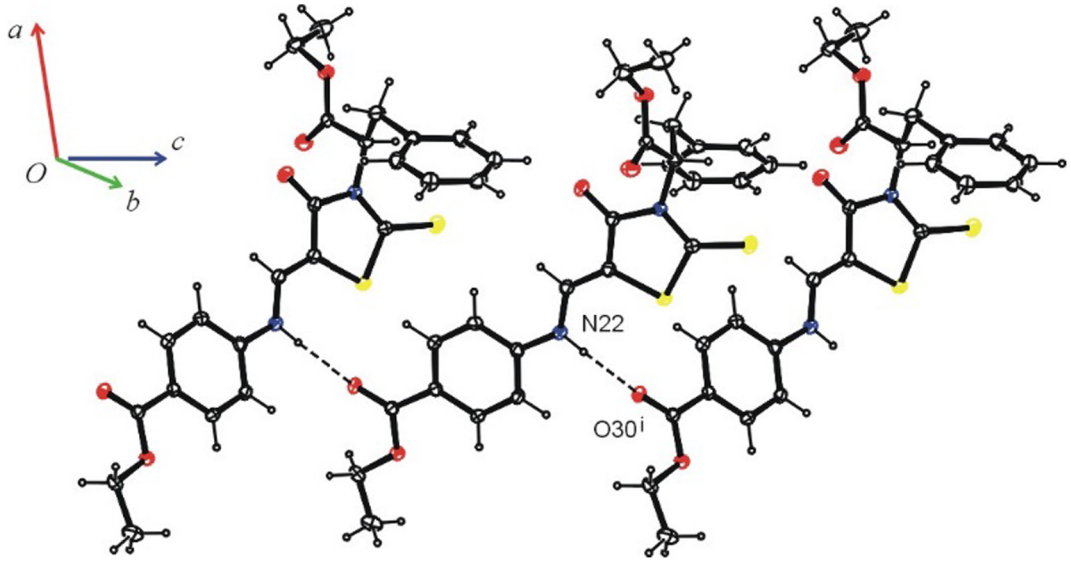

Fig. 4. Part of the crystal structure of **12**, showing the formation of the hydrogen-bonded chain along *c* axis.

Table 1
Antitrypanosomal activity and cytotoxicity of 2-(5-aminomethylene-4-oxo-2-thioxothiazolidin-3-yl)-3-phenylpropionic acid ethyl ester derivatives.

Comp	*Tbb* IC_{50}, μM	*Tbg* IC_{50}, μM	Cytotoxicity on myoblast-derived cell line (L-6) CC_{50}, μM	SI/Tbb	SI/Tbg
3	37.551 ± 15.874	11.592 ± 2.102	175.666 ± 2.102	4.7	15.2
4	2.693 ± 1.687	0.816 ± 0.046	19.938 ± 5.589	7.4	24.4
5	0.513 ± 0.095	0.268 ± 0.082	10.963 ± 0.652	21.4	40.8
6	1.038 ± 0.088	0.447 ± 0.088	11.103 ± 1.757	10.7	24.9
7	0.970 ± 0.187	0.417 ± 0.075	13.456 ± 3.513	13.9	32.3
8	1.931 ± 0.067	1.325 ± 0.217	> 209	> **108**	> **158**
9	3.916 ± 0.803	1.936 ± 0.036	28.803 ± 4.062	7.4	14.9
10	0.679 ± 0.288	0.200 ± 0.010	> 173	> **255**	> **870**
11	10.62 ± 1.46	12.63 ± 0.95	15.43 ± 1.27	1.5	1.2
12	0.091 ± 0.039	0.027 ± 0.006	37.454 ± 20.212	**409.4**	**1396.2**
13	9.653 ± 0.741	13.395 ± 4.178	62.877 ± 16.057	6.5	4.7
14	2.362 ± 0.499	1.851 ± 0.222	8.538 ± 0.398	3.6	4.6
15	23.710 ± 2.356	17.101 ± 4.378	93.622 ± 8.034	3.9	5.5
Pentamidine, nM	1.364 ± 0.464	1.464 ± 0.645	7900,00 ± 282.843	5793,9	5396,9
Nifurtimox	2.389 ± 0.608	4.641 ± 0.725	65.089 ± 2.953	27.2	14.0

were calculated for each cell line: GI_{50} – molar concentration of the compound that inhibits 50% net cell growth; TGI – molar concentration of the compound leading to the total inhibition; and LC_{50} – molar concentration of the compound leading to 50% net cell death (presented in negative logarithm). Furthermore, a mean graph midpoints (MG_MID) were calculated for each of the parameters, giving an average activity parameter over all cell lines for the tested compound. For the MG_MID calculation, insensitive cell lines were included with the highest concentration tested.

Compound **14** inhibited growth of all tested cancer cell lines and showed inhibition activity (GI_{50} < 10 μM) against all 59 human tumor cell lines with average GI_{50}/TGI/LC_{50} values of 2.57/57.27/94.71 μM. Mean pGI_{50}, pTGI, and pLC_{50} values for compound **14** in comparison with standard anticancer agents Tamoxifen, Fluorouracil and Pyrazofurin [40] are given at Fig. 5.

The selectivity index (SI) calculated by dividing the full panel MG-MID (μM) of the compound **14** by their individual subpanel MG-MID of cell line (μM) was considered as a measure of compounds' selectivity

Table 2
Anticancer screening data in concentration 10 μM.

Comp	60 cell lines assay in 1 dose 10 μM concentration				
	Mean growth, %	Range of growth, %	Most sensitive cell line	Positive cytostatic effect[a]	Positive cytotoxic effect[b]
3	88.62	48.01 to 115.75	T-47D (Renal Cancer)	1/59	0/59
4	87.71	58.28 to 107.96	NCI-H522 (Non-Small Cell Lung Cancer)	0/58	0/58
6	82.64	61.45 to 107.11	UACC-62 (Melanoma)	0/58	0/58
8	90.74	56.77 to 108.81	NCI-H522 (Non-Small Cell Lung Cancer)	0/58	0/58
11	100.19	77.21 to 120.59	MOLT-4 (Leukemia)	0/58	0/58
14	3.78	−89.96 to 38.93	Colo 205 (Colon Cancer)	40/59	19/59
15	92.43	64.20 to 114.25	NCI-H522 (Non-Small Cell Lung Cancer)	0/59	0/59

[a] Ratio between number of cell lines with percent growth from 0 to 50 and total number of cell lines.
[b] Ratio between number of cell lines with percent growth of < 0 and total number of cell lines.

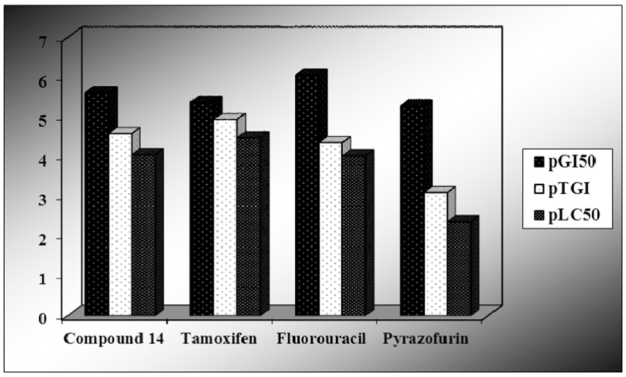

Fig. 5. Anticancer activity of the most active compound **14** in comparison with standard agents.

(Table 3). Ratios between 3 and 6 mean moderate selectivity, ratios greater than 6 indicate high selectivity toward the corresponding cell line, while compounds not meeting either of these criteria are rated nonselective [41]. In this context, the active compound **14** in the present study was found to be nonselective at both the GI_{50} and TGI levels (selectivity indices 0.86–1.26 and 0.56–2.20, respectively) (Table 3). However, the mentioned derivative demonstrated a certain selectivity profile toward some individual cell lines at TGI level. Thus, selectivity indices were 6.14–14.15 for HL(60)-TB (Leukemia), HOP-92 and NCI-H522 (NCS lung cancer), COLO 205 and HT29 (Colon cancer), SF-295 and SF-539 (CNS cancer), SK-MEL-2 and SK-MEL-5 (Melanoma), A498, RXF 393 and UO-31 (Renal cancer), as well as MDA-MB-468 (Breast cancer). At the same time, at GI_{50} level only moderate selectivity was observed for Colon cancer cell line HCT-15 (SI = 4.69).

2.4. COMPARE analysis

NCI's COMPARE algorithm [36–39] allows to predict biochemical mechanisms of action of the novel compounds on the basis of their *in vitro* activity profiles comparing to those of the standard agents. We performed COMPARE computations for the compound **14** against the NCI "Standard Agents" database at the TGI level (Table 4). However, obtained Pearson correlation coefficients (PCC) did not allow to distinguish cytotoxicity mechanism of tested compound with high probability. The compound **14** showed the highest correlation (PCC ≥ 0.50) with transcription inhibitor Actinomycin D, antimetabolite Morpholino-ADR, tubulin polymerization inhibitor Rhizoxin, RNA synthesis inhibitor Mitramycin, pyrimidine biosynthesis inhibitor Dichloroallyl Lawsone and p-glycoprotein inhibitor Thalicarpine.

3. Conclusions

In the present paper new 5-enamine-4-thiazolidinones are described. Trypanocidal activity study of the synthesized compounds allowed to identify 4-{[3-(1-ethoxycarbonyl-2-phenylethyl)-4-oxo-2-thioxothiazolidin-5-ylidenemethyl]-amino}-benzoic acid ethyl ester **12** that was the most active derivative, with the IC_{50} values of 0.091 μM (*Tbb*) and 0.027 μM (*Tbg*) and good cytotoxicity profile against myoblast-derived cell line (L-6) with CC_{50} value of 37.454 μM. Antitumor activity assay of seven synthesized compounds allowed identifying highly active 2-(5-{[5-(2,4-dichlorobenzyl)-thiazol-2-ylamino]-methylene}-4-oxo-2-thioxothiazolidin-3-yl)-3-phenylpropionic acid ethyl ester **14** that inhibited growth of all 59 human tumor cell lines with the average GI_{50} value of 2.57 μM. It should be noted, that the activity type (antitrypanosomal or anticancer) as well as its level significantly depends on the character of enamine fragment in C5 position of thiazolidinone core. Further investigation of such 5-enamine-4-thiazolidinones could lead to more potent compounds as promising candidates for the development of new antitrypanosomal and anticancer chemotherapy.

4. Experimental

4.1. Materials and methods

Commercial reagents were purchased from Merck and used without purification. The starting 2-(4-oxo-2-thioxothiazolidin-3-yl)-3-phenylpropionic acid **1** was obtained according to described procedure [30]. Melting points were measured in open capillary tubes on a BŰCHI B-545 melting point apparatus and are uncorrected. The elemental analyses were performed using the Perkin–Elmer 2400 CHN analyzer. The ^1H and ^{13}C NMR spectra were recorded on Varian Gemini (^1H at 400 and ^{13}C at 100 MHz) instrument in DMSO-d_6 using tetramethylsilane (TMS) as an internal standard. LCMS spectra were obtained using electrospray ionization (ESI) techniques on an Agilent 1100 Series LCMS. The purity of the compounds was checked by thin-layer chromatography performed with Merck Silica Gel 60 F254 aluminum sheets. Spots were detected by their absorption under UV light.

4.2. Chemistry

4.2.1. 2-(5-Ethoxymethylidene-4-oxo-2-thioxothiazolidin-3-yl)-3-phenylpropionic acid ethyl ester (2)

A mixture of **1** (10 mmol) and triethyl orthoformate was refluxed for 2 h in the medium of acetic anhydride (10 mL). The resulting solution was poured onto water, extracted with ethyl acetate, after which the organic layer was distilled off in vacuo. Obtained powder was recrystallized from ethanol. Yield 72%, mp 109–111 °C. ^1H NMR (400 MHz, DMSO-d_6): 1.10 (t, 3H, CH_3), 1.30 (t, 3H, CH_3), 3.50 (d, 2H, CH_2), 4.10 (q, 2H, CH_2), 4.30 (q, 2H, CH_2), 5.70 (t, 1H, CH), 7.00–7.25 (m, 5H, C_6H_5), 7.90 (s, 1H, CH). LCMS (ESI+) *m/z* 366 $(M + H)^+$. Anal. Calcd for $C_{17}H_{19}NO_4S_2$: C, 55.87; H, 5.24; N, 3.83. Found: C, 56.00; H, 5.40; N, 3.70.

4.2.2. 2-(5-Aminomethylene-4-oxo-2-thioxothiazolidin-3-yl)-3-phenylpropionic acid ethyl ester (3)

Equimolar amounts (10 mmol) of **1** and ammonium hydrogen carbonate are placed in the flask and refluxed for 2 h in the ethanol medium. After cooling the reaction mixture, formed precipitate was filtered off and recrystallized from the mixture of ethanol – H_2O (1:1). Yield 54%, mp 102–104 °C. ^1H NMR (400 MHz, DMSO-d_6): 1.10 (t, 3H, CH_3), 3.40 (d, 2H, CH_2), 4.20 (q, 2H, CH_2), 5.70 (t, 1H, CH), 7.00–7.25 (m, 5H, C_6H_5), 7.60 (t, 1H, –CH =), 8.0 (br.s, 2H, NH_2). ^{13}C NMR (100 MHz, DMSO-d_6): 14.5 (CH_3), 33.6 (CH_2), 57.7 (CH), 61.6 (OCH_2), 124.6 (5-$C_{thiaz.}$), 127.0, 128.6, 129.6, 137.2 (CH =), 144.4, 166.5 (C═O), 168.5 (COO), 171.7 (C═S). LCMS (ESI+) *m/z* 337 $(M + H)^+$. Anal. Calcd for $C_{15}H_{16}N_2O_3S_2$: C, 53.55; H, 4.79; N, 8.33. Found: C, 53.70; H, 4.70; N, 8.40.

4.2.3. General procedure for the synthesis of 2-(5-R-aminomethylene-4-oxo-2-thioxothiazolidin-3-yl)-3-phenylpropionic acid ethyl esters (4–15)

A mixture of compound **2** (10 mmol) with the appropriate amine (10 mmol) was refluxed for 2 h in the ethanol medium. The obtained solid products were filtered off, washed with ethanol and recrystallized from ethanol or the mixture of ethanol – H_2O (1:1).

4.2.3.1. 2-(4-Oxo-5-phenylaminomethylene-2-thioxothiazolidin-3-yl)-3-phenylpropionic acid ethyl ester (4).

Yield 56%, mp 182–184 °C. ^1H NMR (400 MHz, DMSO-d_6): 1.17 (t, 3H, J = 6.4 Hz, CH_3), 3.48 (m, 2H, CH_2), 4.15 (q, 2H, J = 6.4 Hz, CH_2), 5.84 (br.s, 1H, CH), 7.12–7.21 (m, 6H, arom), 7.30–7.36 (m, 4H, arom), 8.04 (d, 1H, J = 12.0 Hz, CH), 10.35 (d, 1H, J = 12.0 Hz, NH). ^{13}C NMR (100 MHz, DMSO-d_6): 14.5 (CH_3), 33.6 (CH_2), 58.0 (CH), 61.8 (OCH_2), 117.3, 124.6 (5-$C_{thiaz.}$), 124.7, 127.1, 128.6, 129.6, 130.1, 136.5, 137.0 (CH–), 140.3, 166.8 (C═O), 168.3 (COO), 191.4 (C═S). LCMS (ESI+) *m/z* 413 $(M + H)^+$. Anal.

Table 3
Influence of Compound **14** on the growth of individual tumor cell lines.

Disease	Cell line	GI_{50}, μM	SI (GI_{50})	TGI, μM	SI (TGI)	LC_{50}, μM	SI (LC_{50})
Leukemia	CCRF-CEM	1.87	1.37	> 100.0	–	> 100.0	
	HL-60 (TB)	2.29	1.12	7.06	6.70	> 100.0	
	K-562	2.03	1.27	> 100.0	–	> 100.0	
	MOLT-4	3.29	0.78	> 100.0	–	> 100.0	
	RPMI-8226	2.12	1.21	> 100.0	–	> 100.0	
	SR	3.98	0.78	> 100.0	–	> 100.0	
	MG_MID	**2.60**	**0.99**	**84.51**	**0.56**	**> 100**	**–**
NSC lung cancer	A549/ATCC	3.86	0.67	> 100.0	–	> 100.0	–
	EKVX	2.07	1.24	> 100.0	–	> 100.0	–
	HOP-62	2.96	0.87	8.12	5.82	> 100.0	–
	HOP-92	1.65	1.56	6.22	7.60	> 100.0	–
	NCI-H266	3.29	0.78	> 100.0	–	> 100.0	–
	NCI-H23	1.90	1.35	12.4	3.81	> 100.0	–
	NCI-H322M	3.38	0.76	37.2	1.27	> 100.0	–
	NCI-H460	2.09	1.23	12.4	3.81	> 100.0	–
	NCI-H522	1.31	1.96	5.70	8.29	> 100.0	–
	MG_MID	**2.50**	**1.03**	**42.45**	**1.11**	**> 100**	**–**
Colon cancer	COLO 205	1.66	1.55	3.34	14.15	6.72	14.09
	HCC-2998	2.54	1.01	42.3	1.12	> 100.0	–
	HCT-116	2.03	1.27	11.5	4.11	> 100.0	–
	HCT-15	0.548	4.69	> 100.0	–	> 100.0	–
	HT29	2.24	1.15	7.70	6.14	> 100.0	–
	KM12	1.84	1.40	11.6	4.08	> 100.0	–
	SW-620	3.45	0.74	> 100.0	–	> 100.0	–
	MG_MID	**2.04**	**1.26**	**39.49**	**1.20**	**86.87**	**1.09**
CNS cancer	SF-268	2.42	1.06	64.8	0.73	> 100.0	–
	SF-295	2.31	1.11	6.84	6.91	> 100.0	–
	SF-539	2.58	1.00	6.95	6.90	44.3	2.14
	SNB-19	5.05	0.51	> 100.0	–	> 100.0	–
	SNB-75	2.81	0.91	21.4	2.21	> 100.0	–
	U251	2.51	1.02	15.0	3.15	> 100.0	–
	MG_MID	**2.95**	**0.87**	**35.83**	**1.32**	**90.55**	**1.05**
Melanoma	LOX IMVI	3.44	0.74	16.5	2.86	> 100.0	–
	MALME-3M	2.77	0.93	9.25	5.11	> 100.0	–
	M14	3.02	0.85	16.7	2.83	> 100.0	–
	MDA-MB-435	3.38	0.76	> 100.0	–	> 100.0	–
	SK-MEL-2	1.31	1.96	5.68	8.32	> 100.0	–
	SK-MEL-28	2.61	0.98	26.4	1.79	> 100.0	–
	SK-MEL-5	1.52	1.69	4.13	10.99	17.0	5.57
	UACC-257	2.72	0.94	8.57	5.52	> 100.0	–
	UACC-62	1.63	1.58	6.36	7.50	> 100.0	–
	MG_MID	**2.49**	**1.03**	**21.51**	**2.20**	**90.78**	**1.04**
Ovarian cancer	IGROV1	3.73	0.69	71.5	0.66	> 100.0	–
	OVCAR-3	2.84	0.90	9.96	4.75	> 100.0	–
	OVCAR-4	3.22	0.80	> 100.0	–	> 100.0	–
	OVCAR-5	4.20	0.61	> 100.0	–	> 100.0	–
	OVCAR-8	2.07	1.24	> 100.0	–	> 100.0	–
	NCI/ADR-RES	2.56	1.00	15.1	3.13	> 100.0	–
	SK-OV-3	2.38	1.08	11.8	4.01	> 100.0	–
	MG_MID	**3.00**	**0.86**	**55.34**	**0.85**	**> 100**	**–**
Renal cancer	786–0	3.15	0.82	> 100.0	–	> 100.0	–
	A498	1.58	1.63	7.64	6.19	> 100.0	–
	ACHN	2.92	0.88	> 100.0	–	> 100.0	–
	CAKI-1	1.71	1.50	> 100.0	–	> 100.0	–
	RXF 393	2.56	1.00	6.70	7.06	> 100.0	–
	SN12C	1.59	1.62	> 100.0	–	> 100.0	–
	UO-31	1.97	1.30	5.31	8.90	20.6	4.60
	MG_MID	**2.21**	**1.16**	**59.95**	**0.79**	**88.66**	**1.07**
Prostate Cancer	PC-3	2.08	1.24	> 100.0	–	> 100.0	–
	DU-145	3.90	0.66	> 100.0	–	> 100.0	–
	MG_MID	**2.99**	**0.86**	**> 100**	**–**	**> 100**	**–**
Breast cancer	MCF7	2.36	1.09	> 100.0	–	> 100.0	–
	MDA-MB-231/ATCC	3.88	0.66	21.4	2.21	> 100.0	–
	HS 578T	3.62	0.71	41.1	1.15	> 100.0	–
	BT-549	2.37	1.08	8.23	5.74	> 100.0	–
	T-47D	2.16	1.19	8.73	5.41	> 100.0	–
	MDA-MB-468	2.48	1.03	7.35	6.43	> 100.0	–
	MG_MID	**2.81**	**0.91**	**31.14**	**1.52**	**> 100**	**–**
MG_MID		**2.57**		**47.27**		**94.71**	

Table 4
COMPARE analysis results for compound **14** at TGI level.

Rank	PCC[a]	Target	Target vector NSC	Target mechanism of action[b]
1	0.592	Actinomycin D	S3053	transcription inhibitor
2	0.545	Morpholino-ADR	S354646	antimetabolite
3	0.539	Rhizoxin	S332598	tubulin polymerization inhibitor
4	0.512	Mitramycin	S24559	RNA synthesis inhibitor
5	0.512	Dichloroallyl Lawsone	S126771	pyrimidine biosynthesis inhibitor
6	0.503	Thalicarpine	S68075	p-glycoprotein inhibitor

[a] Only correlations with PCC ≥ 0.50 were selected, as significant.
[b] Putative mechanisms of action were identified with the use of literature sources.

Calcd for $C_{21}H_{20}N_2O_3S_2$: C, 61.14; H, 4.89; N, 6.79. Found: C, 61.30; H, 4.80; N, 6.70.

*4.2.3.2. 2-{5-[(4-Chlorophenylamino)-methylene]-4-oxo-2-thioxothiazolidin-3-yl}-3-phenylpropionic acid ethyl ester (**5**)*. Yield 68%, mp 202–204 °C. ^{1}H NMR (400 MHz, DMSO-d_6): 1.10 (t, 3H, CH_3), 3.50 (d, 2H, CH_2), 4.10 (q, 2H, CH_2), 5.80 (t, 1H, CH), 7.00–7.20 (m, 5H, C_6H_5), 7.30–7.50 (m, 4H, C_6H_4), 8.00 (d, 1H, CH), 10.40 (d, 1H, NH). ^{13}C NMR (100 MHz, DMSO-d_6): 14.5 (CH_3), 33.4 (CH_2), 58.0 (CH), 61.8 (OCH_2), 119.0, 127.1 (5-$C_{thiaz.}$), 128.3, 128.6, 129.6, 129.9, 136.2, 137.0 (CH═), 139.4, 166.7, 168.2 (C═O), 187.5 (COO), 191.4 (C═S). LCMS (ESI+) *m/z* 447/449 $(M + H)^+$. Anal. Calcd for $C_{21}H_{19}ClN_2O_3S_2$: C, 56.43; H, 4.28; N, 6.27. Found: C, 56.40; H, 4.30; N, 6.30.

*4.2.3.3. 2-{5-[(4-Fluorophenylamino)-methylene]-4-oxo-2-thioxothiazolidin-3-yl}-3-phenylpropionic acid ethyl ester (**6**)*. Yield 61%, mp 189–191 °C. ^{1}H NMR (400 MHz, DMSO-d_6): 1.15 (t, 3H, J = 6.8 Hz, CH_3), 3.47 (m, 2H, CH_2), 4.14 (q, 2H, J = 6.8 Hz, CH_2), 5.80 (br.s, 1H, CH), 7.16–7.20 (m, 5H, arom), 7.20–7.40 (m, 4H, arom), 8.02 (d, 1H, J = 12.1 Hz, CH), 10.36 (d, 1H, J = 12.1 Hz, NH). ^{13}C NMR (100 MHz, DMSO-d_6): 14.5 (CH_3), 33.6 (CH_2), 58.0 (CH), 61.8 (OCH_2), 116.6, 116.8, 127.1 (5-$C_{thiaz.}$), 128.6, 129.6, 137.0 (CH =), 159.3 (d, J = 240.0 Hz), 166.7, 168.3 (C═O); 180.6, 187.6 (COO); 191.3, 194.0 (C═S). LCMS (ESI+) *m/z* 431 $(M + H)^+$. Anal. Calcd for $C_{21}H_{19}FN_2O_3S_2$: C, 58.59; H, 4.45; N, 6.51. Found: C, 58.70; H, 4.50; N, 6.60.

*4.2.3.4. 2-{5-[(4-Chloro-2-nitrophenylamino)-methylene]-4-oxo-2-thioxothiazolidin-3-yl}-3-phenylpropionic acid ethyl ester (**7**)*. Yield 62%, mp 240–242 °C. ^{1}H NMR (400 MHz, DMSO-d_6): 1.18 (t, 3H, J = 6.8 Hz, CH_3), 3.53 (m, 2H, CH_2), 4.17 (q, 2H, J = 6.8 Hz, CH_2), 5.92 (m, 1H, CH), 7.17–7.19 (m, 3H, arom), 7.21 (d, 2H, J = 7.0 Hz, arom), 7.78 (d, 1H, J = 9.0 Hz, arom), 7.92 (d, 1H, J = 9.0 Hz, arom.), 8.26 (s, 1H, arom), 8.51 (d, 1H, J = 12.1 Hz, CH), 12.20 (d, 1H, J = 12.1 Hz, NH). ^{13}C NMR (100 MHz, DMSO-d_6): 14.5 (CH_3), 33.4 (CH_2), 57.9 (CH), 62.0 (OCH_2), 98.5, 119.3, 126.1, 127.2 (5-$C_{thiaz.}$), 128.7, 129.6, 135.1, 136.4, 136.5, 136.8, 137.4 (CH═), 166.7, 168.0 (C═O), 171.8 (COO), 187.5 (C═S). LCMS (ESI+) *m/z* 492/494 $(M + H)^+$. Anal. Calcd for $C_{21}H_{18}ClN_3O_5S_2$: C, 51.27; H, 3.69; N, 8.54. Found: C, 51.20; H, 3.60; N, 8.60.

*4.2.3.5. 2-{5-[(5-Chloro-2-methoxyphenylamino)-methylene]-4-oxo-2-thioxothiazolidin-3-yl}-3-phenylpropionic acid ethyl ester (**8**)*. Yield 60%, mp 210–213 °C. ^{1}H NMR (400 MHz, DMSO-d_6): 1.17 (t, 3H, J = 6.0 Hz, CH_3), 3.47–3.51 (m, 2H, CH_2), 3.85, 3.92 (2*s, 3H, CH_3), 4.15 (m, 2H, CH_2), 5.82, 5.89 (2*br.s, 1H, CH), 7.10–7.21 (m, 7H, arom), 7.40, 7.52 (2*s. 1H, arom), 7.91, 8.43 (br.s; d, J = 12.6 Hz; 1H, CH), 9.99, 10.53 (br.s; d, J = 12.6 Hz; 1H, NH). ^{13}C NMR (100 MHz, DMSO-d_6): 14.5 (CH_3), 33.7 (CH_2), 56.7 (OCH_3), 57.1, 57.9 (CH), 61.8, 61.9 (OCH_2), 113.7, 114.1, 114.3, 124.3, 125.2, 125.7, 127.1, 127.2 (5-$C_{thiaz.}$), 128.6, 128.7, 129.6, 136.9, 137.0 (CH═), 139.0, 146.8, 166.9, 167.0, 168.1 (C═O), 168.3 (COO), 191.9 (C═S). LCMS (ESI+) *m/z* 477/479 $(M + H)^+$. Anal. Calcd for $C_{22}H_{21}ClN_2O_4S_2$: C, 55.40; H, 4.44; N, 5.87. Found: C, 55.50; H, 4.30; N, 5.90.

*4.2.3.6. 2-{4-Oxo-5-[(4-sulfamoylphenylamino)-methylene]-2-thioxothiazolidin-3-yl}-3-phenylpropionic acid ethyl ester (**9**)*. Yield 53%, mp 231–234 °C. ^{1}H NMR (400 MHz, DMSO-d_6): 1.16 (t, 3H, J = 6.4 Hz, CH_3), 3.48 (br.s, 2H, CH_2), 4.15 (q, 2H, J = 6.4 Hz, CH_2), 5.85 (br.s, 1H, CH), 7.16–7.19 (m, 3H, arom), 7.21 (d, 2H, J = 7.0 Hz, arom), 7.29 (br.s, 2H, NH_2), 7.47 (d, 2H, J = 7.5 Hz, arom.), 7.77 (d, 2H, J = 7.5 Hz, arom.), 8.11 (br.s, 1H, CH), 10.53 (br.s, 1H, NH). ^{13}C NMR (100 MHz, DMSO-d_6): 14.5 (CH_3), 33.6 (CH_2), 58.1 (CH), 61.8 (OCH_2), 117.0, 127.1 (5-$C_{thiaz.}$), 127.7, 127.9, 128.7, 129.6, 135.6, 136.9 (CH═), 139.3, 143.1, 166.8 (C═O), 168.2 (COO), 191.6 (C═S). LCMS (ESI+) *m/z* 492 $(M + H)^+$. Anal. Calcd for $C_{21}H_{21}N_3O_5S_3$: C, 51.31; H, 4.31; N, 8.55. Found: C, 51.40; H, 4.40; N, 6.60.

*4.2.3.7. 2-(5-{[2-Methyl-5-(morpholine-4-sulfonyl)phenylamino]-methylene}-4-oxo-2-thioxothiazolidin-3-yl)-3-phenylpropionic acid ethyl ester (**10**)*. Yield 64%, mp 208–210 °C. ^{1}H NMR (400 MHz, DMSO-d_6): 1.17 (br.s, 3H, CH_3); 2.36, 2.40 (2*s, 3H, CH_3); 3.40–3.65 (m, 10*H*, CH_2, morpholine); 4.15 (br.s, 2H, CH_2); 5.83 (m, 1H, CH); 7.19–7.90 (m, 8H, arom); 8.56 (br.s, 1H, CH); 9.97, 10.20 (2*br.s, 1H, NH). LCMS (ESI+) *m/z* 576 $(M + H)^+$. Anal. Calcd for $C_{26}H_{29}N_3O_6S_3$: C, 54.24; H, 5.08; N, 7.30. Found: C, 54.30; H, 5.00; N, 7.40.

*4.2.3.8. 2-{5-[(4-Ethylsulfanylthiosulfonylphenylamino)-methylene]-4-oxo-2-thioxothiazolidin-3-yl}-3-phenylpropionic acid ethyl ester (**11**)*. Yield 60%, mp 236–238 °C. ^{1}H NMR (400 MHz, DMSO-d_6): 1.12–1.21 (m, 6H, 2CH_3), 3.0 (q, 2H, J = 6.8 Hz, CH_2), 3.42 (m, 2H, CH_2), 4.13 (q, 2H, J = 7.0 Hz, CH_2), 5.82 (m, 1H, CH), 7.05–7.20 (m, 5H, arom), 7.51 (d, 2H, J = 8.2 Hz, arom.), 7.55 (d, 2H, J = 8.2 Hz, arom), 8.20 (m, 1H, CH), 10.40 (br.s, 1H, NH). ^{13}C NMR (100 MHz, DMSO-d_6): 14.5 (CH_3), 14.8 ($\underline{CH_3}CH_2S$), 30.8 (CH_2S), 33.6 (CH_2), 58.1 (CH), 61.9 (OCH_2), 117.3, 127.2 (5-$C_{thiaz.}$), 128.7, 129.2, 129.6, 134.9, 136.9 (CH═), 138.6, 138.8, 145.2, 166.9 (C═O), 168.1 (COO), 191.6 (C═S). LCMS (ESI+) *m/z* 537 $(M + H)^+$. Anal. Calcd for $C_{23}H_{24}N_2O_5S_4$: C, 51.47; H, 4.51; N, 5.22. Found: C, 51.40; H, 4.60; N, 5.30.

*4.2.3.9. 4-{[3-(1-Ethoxycarbonyl-2-phenylethyl)-4-oxo-2-thioxothiazolidin-5-ylidenemethyl]-amino}-benzoic acid ethyl ester (**12**)*. Yield 71%, mp 196–198 °C. ^{1}H NMR (400 MHz, DMSO-d_6): 1.17 (br.s, 3H, CH_3), 1.31 (br.s, 3H, CH_3), 3.48 (br.s, 2H, CH_2), 4.15 (br.s, 2H, CH_2), 4.28 (br.s, 2H, CH_2), 5.85 (br.s, 1H, CH), 7.16–7.21 (m, 5H, arom), 7.43 (d, 2H, J = 7.7 Hz, arom), 7.92 (d, 2H, J = 7.7 Hz, arom), 8.11 (br.s, 1H, CH), 10.54 (br.s, 1H, NH). ^{13}C NMR (100 MHz, DMSO-d_6): 14.5 (CH_3), 14.7 (CH_3), 33.6 (CH_2), 58.1 (CH), 61.0 (OCH_2), 61.8 (OCH_2), 95.8, 116.7, 125.1, 127.1 (5-$C_{thiaz.}$), 128.7, 129.6, 131.4, 135.3, 136.9 (CH═), 144.4, 165.6, 166.8 (C═O), 168.2 (COO), 191.6 (C═S). LCMS (ESI+) *m/z* 485 $(M + H)^+$. Anal. Calcd for $C_{24}H_{24}N_2O_5S_2$: C, 59.49; H, 4.99; N, 5.78. Found: C, 59.40; H, 4.80; N, 5.80.

*4.2.3.10. 2-[4-Oxo-5-(thiazol-2-ylaminomethylene)-2-thioxothiazolidin-3-yl]-3-phenylpropionic acid ethyl ester (**13**)*. Yield 64%, mp 218–220 °C. ^{1}H NMR (400 MHz, DMSO-d_6): 1.10 (t, 3H, CH_3), 3.60 (d, 2H, CH_2), 4.10 (q, 2H, CH_2), 5.90 (t, 1H, CH), 7.10–7.50 (m, 5H, C_6H_5), 7.60 (d, 2H, thiazole), 7.90 (d, 2H, thiazole), 8.00 (s, 1H, CH), 10.00 (s, 1H, NH). ^{13}C NMR (100 MHz, DMSO-d_6): 14.5 (CH_3), 33.5 (CH_2), 58.1 (CH), 61.9 (OCH_2), 107.0 (5-$C_{thiazole}$), 127.2 (5-$C_{thiaz.}$), 128.7, 129.6, 134.8 (4-$C_{thiazole}$), 136.8, 146.2 (CH═), 148.3, 157.9 (C═O), 167.1 (2-$C_{thiazole}$), 168.1 (COO), 192.0 (C═S). LCMS (ESI+) *m/z* 420 $(M + H)^+$. Anal. Calcd for $C_{18}H_{17}N_3O_3S_3$: C, 51.53; H, 4.08; N,

10.02. Found: C, 51.60; H, 4.00; N, 10.10.

*4.2.3.11. 2-(5-{[5-(2,4-Dichlorobenzyl)-thiazol-2-ylamino]-methylene}-4-oxo-2-thioxothiazolidin-3-yl)-3-phenylpropionic acid ethyl ester (**14**)*. Yield 63%, mp 226–228 °C. ^{1}H NMR (400 MHz, DMSO-d_6): 1.10 (t, 3H, CH_3), 3.60 (d, 2H, CH_2), 4.00–4.10 (m, 4H,2*CH_2), 5.90 (t, 1H, CH), 7.00–7.40 (m, 9H, C_6H_3, C_6H_5, thiazole), 7.90 (d, 1H, CH), 11.30 (s, 1H, NH). LCMS (ESI+) *m/z* 578/580 $(M + H)^+$. Anal. Calcd for $C_{25}H_{21}Cl_2N_3O_3S_3$: C, 51.90; H, 3.66; N, 7.26. Found: C, 51.80; H, 3.70; N, 7.15.

*4.2.3.12. 2-{4-Oxo-2-thioxo-5-[(4H-[1,2,4]triazol-3-ylamino)methylene]-thiazolidin-3-yl}-3-phenylpropionic acid ethyl ester (**15**)*.. Yield 54%, mp 198–200 °C. ^{1}H NMR (400 MHz, DMSO-d_6): 1.10 (t, 3H, CH_3), 3.40 (d, 2H, CH_2), 4.10 (q, 2H, CH_2), 5.80 (t, 1H, CH), 7.10–7.30 (m, 5H, C_6H_5), 8.10 (d, 1H, CH), 8.50 (s, 1H, CH, triazole), 11.30 (d, 1H, NH), 13.90 (s, 1H, NH, triazole). ^{13}C NMR (100 MHz, DMSO-d_6): 14.5 (CH_3), 33.4 (CH_2), 58.1 (CH), 61.8 (OCH_2), 121.0, 127.1 (5-$C_{thiaz.}$), 128.6, 129.6, 140.7 (5-$C_{triazole}$), 143.9 (CH=), 145.0, 151.1, 167.3 (C=O), 168.2 (3-$C_{triazole}$), 178.9 (COO), 195.5 (C=S). LCMS (ESI+) *m/z* 404 $(M + H)^+$. Anal. Calcd for $C_{17}H_{17}N_5O_3S_2$: C, 50.61; H, 4.25; N, 17.36. Found: C, 50.60; H, 4.30; N, 17.40.

*4.2.4. Crystal structure determination of compounds **2**, **3** and **12***

The molecular illustrations were drawn using ORTEP-3 for Windows [42]. Software used to prepare the material for publication was WINGX [42], OLEX [43] and PLATON [44]. The supplementary crystallographic data have been deposited at the Cambridge Crystallographic Data Centre (CCDC), 12 Union ROAD, Cambridge CB2 1EZ (UK), Tel.: (ţ44) 1223/336e408, Fax: (ţ44) 1223/336-033, E-mail: deposit@ccdc.cam.ac.uk, http://www.ccdc.cam.ac.uk, deposition No. CCDC 1,872,547 (compound **2**), CCDC 1,872,546 (compound **3**) and CCDC 1872545 (compound **12**).

*4.2.4.1. Crystal structure determination of 2-(5-ethoxymethylidene-4-oxo-2-thioxothiazolidin-3-yl)-3-phenylpropionic acid ethyl ester (**2**). Crystal data*. $C_{17}H_{19}NO_4S_2$, Mr = 365.45, monoclinic, space group *C2/c*, *a* = 17.9894(4), *b* = 8.4463(2), *c* = 24.2633(8) Å, *β* = 98.403(3), *V* = 3647.08(17) Å^3, *Z* = 8, D_{calc} = 1.331 g/cm^3, *μ* = 2.823 mm^{-1}, *T* = 130.0(1) K.

Data collection. A red lath crystal (EtOH) of 0.35 × 0.13 × 0.04 mm was used to record 19212 (Cu *Kα*-radiation, θ_{max} = 76.38°) intensities on a Rigaku SuperNova Dual Atlas diffractometer [45] using mirror monochromatized Cu Kα radiation from a high-flux microfocus source (λ = 1.54178 Å). Accurate unit cell parameters were determined by least-squares techniques from the *θ* values of 7168 reflections, *θ* range 3.64–76.16°. The data were corrected for Lorentz, polarization and for absorption effects [45]. The 3809 total unique reflections (R_{int} = 0.0345) were used for structure determination.

Structure solution and refinement. The structure was solved by dual-space algorithm (SHELXT) [46], and refined against F^2 for all data (SHELXL-97) [47]. The H atoms were positioned geometrically and were refined using a riding model, with C—H = 0.98 Å (CH_3), 0.99 Å (CH_2), 1.00 (C*sp*^{3}H), 0.95 Å (C$_{ar}$H) and U_{iso}(H) = 1.2U_{eq}(C) or 1.5U_{eq}(C) for methyl H atoms. The methyl groups were refined as a rigid group, which were allowed to rotate. Non-hydrogen atoms of the disordered parts within molecules of compound **2** were obtained from difference Fourier maps. During refinement, the atomic displacement ellipsoids of the corresponding atoms in the alternative positions were constrained to be identical. Corresponding bond distances within the disordered components were restrained to be similar. Final refinement converged with *R* = 0.0412 (for 3179 data with $F^2 > 4\sigma(F^2)$), w*R* = 0.1181 (on F^2 for all data), and *S* = 1.044 (on F^2 for all data). The largest difference peak and hole was 0.235 and −0.366 eÅ^3.

*4.2.4.2. Crystal structure determination of ethyl 2-(5-aminomethylene-4-oxo-2-thioxothiazolidin-3-yl)-3-phenylpropionic acid ethyl ester (**3**). Crystal data*. $C_{15}H_{16}N_2O_3S_2$, Mr = 336.42, monoclinic, space group $P2_1/c$, *a* = 12.8232(2), *b* = 9.1569(2), *c* = 29.0742(7) Å, *β* = 94.824(2)°, *V* = 3401.82(12) Å^3, *Z* = 8, D_{calc} = 1.314 g/cm^3, *μ* = 2.953 mm^{-1}, *T* = 130.0(1) K.

Data collection. A yellow lath crystal (MeOH) of 0.23 × 0.14 × 0.04 mm was used to record 26,789 (Cu *Kα*-radiation, θ_{max} = 76.81°) intensities on a Rigaku SuperNova Dual Atlas diffractometer [48] using mirror monochromatized Cu Kα radiation from a high-flux microfocus source (λ = 1.54178 Å). Accurate unit cell parameters were determined by least-squares techniques from the *θ* values of 14,584 reflections, *θ* range 3.00–76.19°. The data were corrected for Lorentz, polarization and for absorption effects [48]. The 9581 total unique reflections were used for structure determination.

Structure solution and refinement. The structure was solved by dual-space algorithm (SHELXT) [46], and refined against F^2 for all data (SHELXL-97) [47]. The positions of the H atoms bonded to N atom were obtained from the difference Fourier maps and were refined freely. The remaining H atoms were positioned geometrically and were refined with a riding model, with C—H = 0.98 Å (CH_3), 0.99 Å (CH_2), 1.00 (C*sp*^{3}H), 0.95 Å (C$_{ar}$H) and U_{iso}(H) = 1.2U_{eq}(C)) or 1.5U_{eq}(C) for methyl H atoms. The methyl groups were refined as a rigid group, which were allowed to rotate. Final refinement converged with *R* = 0.0419 (for 8407 data with $F^2 > 4\sigma(F^2)$), w*R* = 0.1342 (on F^2 for all data), and *S* = 1.066 (on F^2 for all data). The largest difference peak and hole was 0.352 and −0.333 eÅ^3.

*4.2.4.3. Crystal structure determination of ethyl 4-{[3-(1-ethoxycarbonyl-2-phenylethyl)-4-oxo-2-thioxothiazolidin-5-ylidenemethyl]-amino}-benzoic acid ethyl ester (**12**). Crystal data*. $C_{24}H_{24}N_2O_5S_2$, Mr = 484.57, monoclinic, space group $P2_1/c$, *a* = 18.8461(4), *b* = 8.2841(2), *c* = 15.0392(3) Å, *β* = 99.644(2)°, *V* = 2314.78(9) Å^3, *Z* = 4, D_{calc} = 1.390 g/cm^3, *μ* = 2.416 mm^{-1}, *T* = 130.0(1) K.

Data collection. A pale-yellow plate crystal (DMF) of 0.23 × 0.14 × 0.04 mm was used to record 24,544 (Cu *Kα*-radiation, θ_{max} = 76.33°) intensities on a Rigaku SuperNova Dual Atlas diffractometer [48] using mirror monochromatized Cu Kα radiation from a high-flux microfocus source (λ = 1.54178 Å). Accurate unit cell parameters were determined by least-squares techniques from the *θ* values of 9195 reflections, *θ* range 3.43–75.76°. The data were corrected for Lorentz, polarization and for absorption effects [48]. The 4833 total unique reflections were used for structure determination.

Structure solution and refinement. The structure was solved by dual-space algorithm (SHELXT) [46], and refined against F^2 for all data (SHELXL-97) [47]. The position of the H atom bonded to N atom was obtained from the difference Fourier map and was refined freely. The remaining H atoms were positioned geometrically and were refined within the riding model approximation: C—H = 0.98 Å (CH_3), 0.99 Å (CH_2), 1.00 (C*sp*^{3}H), 0.95 Å (C$_{ar}$H) and U_{iso}(H) = 1.2U_{eq}(C)) or 1.5U_{eq}(C) for methyl H atoms. The methyl groups were refined as a rigid group, which were allowed to rotate. Final refinement converged with *R* = 0.0487 (for 4257 data with $F^2 > 4\sigma(F^2)$), w*R* = 0.1164 (on F^2 for all data), and *S* = 1.092 (on F^2 for all data). The largest difference peak and hole was 0.596 and −0.373 eÅ^3.

4.3. Pharmacology

4.3.1. Antitrypanosomal activity assay

Bloodstream forms of *Tbb* strain 90–13 and *Tbg* Feo strain were cultured in HMI9 medium supplemented with 10% FCS at 37 °C under an atmosphere of 5% CO_2 [49]. In all experiments, log-phase parasite cultures were harvested by centrifugation at 3000*g* and immediately used. Drug assays were based on the conversion of a redox-sensitive dye (resazurin) to a fluorescent product by viable cells as previously described [50]. Drug stock solutions were prepared in pure DMSO. *Trypanosoma brucei* bloodstream forms (10^5 cells/ml) were cultured in 96-

well plates either in the absence or in the presence of different concentrations of inhibitors in a final volume of 200 µl. After a 72-h incubation, resazurin solution was added in each well at the final concentration of 45 µM and fluorescence was measured at 530 nm and 590 nm absorbance after a further 4-h incubation. The percentage of inhibition of parasite growth rate was calculated by comparing the fluorescence of parasites maintained in the presence of drug to that of in the absence of drug. DMSO was used as control. Concentration inhibiting 50% of parasite growth (IC_{50}) was determined from the dose-response curve with a drug concentrations ranging from 10 µg/ml to 0.625 µg/ml and presented in µM. IC_{50} value is the mean ± the standard deviation of three independent experiments.

4.3.2. In vitro cytotoxicity assay on mammalian cell

Cytotoxicity was evaluated by using a rat myoblast-derived cell line (L-6). Assays were performed in 96-well plates in RPMI medium containing 25 mM HEPES, pH 7.3, 10% foetal calf serum under 5% CO_2 atmosphere, at 37 °C. After trypsin treatment, L-6 cells were seeded at 5000 cells per well in 100 µl. After 24 h incubation, cells were washed and two-fold dilutions of drug were added (200 µl per well). Drug stock solutions were prepared in pure DMSO. The final DMSO concentration in the cultures remained below 1%. Control cultures were constituted of cultures treated with pure DMSO instead of drug. The cytotoxicity assay was based on the conversion of a redox sensitive dye (resazurin) to a fluorescent product by viable cells [51]. After 5 days of incubation, resazurin solution was added in each well at the final concentration of 45 µM. Fluorescence was measured at 530 nm excitation and 590 nm emission wavelengths after further 4-h incubation. The percentage of inhibition of cell growth was calculated by comparing the fluorescence of cells maintained in the presence of drug to that of in the absence of drug. IC_{50}s were determined from the dose-response curves with drug concentrations ranging from 10 µg/ml to 10 ng/ml. IC_{50} value is the mean ± the standard deviation of three independent experiments.

4.3.3. In vitro anticancer assay

Primary anticancer assay was performed on a panel of approximately sixty human tumor cell lines derived from nine neoplastic diseases, in accordance with the protocol of the Drug Evaluation Branch, National Cancer Institute, Bethesda [36–39]. Tested compounds were added to the culture at a single concentration (10^{-5} M) and the cultures were incubated for 48 h. End point determinations were made with a protein binding dye, sulforhodamine B (SRB). Results for each tested compound were reported as the percent of growth of the treated cells when compared to the untreated control cells. The percentage growth was evaluated spectrophotometrically versus controls not treated with test agents. The cytotoxic and/or growth inhibitory effects of the most active selected compounds were tested *in vitro* against the full panel of human tumor cell lines at concentrations ranging from 10^{-4} to 10^{-8} M. 48-h continuous drug exposure protocol was followed and an SRB protein assay was used to estimate cell viability or growth.

Using absorbance measurements [time zero (Tz), control growth in the absence of drug (C), and test growth in the presence of drug (Ti)], the percentage growth was calculated for each drug concentration. Percentage growth inhibition was calculated as:

$[(Ti - Tz)/(C - Tz)] \times 100$ for concentrations for which $Ti \geq Tz$,

$[(Ti - Tz)/Tz] \times 100$ for concentrations for which $Ti < Tz$.

Dose response parameters (GI_{50}, TGI) were calculated for each compound. Growth inhibition of 50% (GI_{50}) was calculated from $[(Ti - Tz)/(C - Tz)] \times 100 = 50$, which is the drug concentration resulting in a 50% lower net protein increase in the treated cells (measured by SRB staining) as compared to the net protein increase seen in the control cells. The drug concentration resulting in total growth inhibition (TGI) was calculated from $Ti = Tz$. Values were calculated for each of these parameters if the level of activity was reached; however, if the effect was not reached or was excessive, the value for that parameter was expressed as more or less than the maximum or minimum concentration tested. The lowest values were obtained with the most sensitive cell lines. Compounds having GI_{50} values ≤100 µM were declared to be active.

Acknowledgements

We are grateful to Dr. V.L. Narayanan from Drug Synthesis and Chemistry Branch, National Cancer Institute, Bethesda, MD, USA, for *in vitro* evaluation of anticancer activity.

Appendix A. Supplementary material

Supplementary data to this article can be found online at https://doi.org/10.1016/j.bioorg.2019.01.045.

References

[1] World Health Organization. Trypanosomiasis, Human African (Sleeping sickness), 2016. Fact sheet < http://www.who.int/mediacentre/factsheets/fs259/en/ > (accessed 1 November 2018).
[2] P.P. Simarro, A. Diarra, J.A.R. Postigo, J.R. Franco, J.G. Jannin, The human African trypanosomiasis control and surveillance programme of the World Health Organization 2000–2009: the way forward, PLoS Negl. Trop. Dis. 5 (2) (2011) e1007, https://doi.org/10.1371/journal.pntd.0001007.
[3] P.G. Kennedy, Clinical features, diagnosis, and treatment of human African trypanosomiasis (sleeping sickness), The Lancet Neurol. 12 (2) (2013) 186–194, https://doi.org/10.1016/S1474-4422(12)70296-X.
[4] D. Kaminskyy, A. Kryshchyshyn, R. Lesyk, Recent developments with rhodanine as a scaffold for drug discovery, Expert Opin. Drug Discov. 12 (12) (2017) 1233–1252, https://doi.org/10.1080/17460441.2017.1388370.
[5] D. Kaminskyy, A. Kryshchyshyn, R. Lesyk, 5-Ene-4-thiazolidinones – an efficient tool in medicinal chemistry, Eur. J. Med. Chem. 140 (2017) 542–594, https://doi.org/10.1016/j.ejmech.2017.09.031.
[6] D. Havrylyuk, O. Roman, R. Lesyk, Synthetic approaches, structure activity relationship and biological applications for pharmacologically attractive pyrazole/pyrazoline–thiazolidine–based hybrids, Eur. J. Med. Chem. 113 (2016) 145–166, https://doi.org/10.1016/j.ejmech.2016.02.030.
[7] R.B. Lesyk, B.S. Zimenkovsky, D.V. Kaminskyy, A.P. Kryshchyshyn, D.Ya Havrylyuk, D.V. Atamanyuk, I. Yu Subtel'na, D.V. Khylyuk, Thiazolidinone motif in anticancer drug discovery. Experience of DH LNMU medicinal chemistry scientific group, Biopolym. Cell. 27 (2) (2011) 107–117, https://doi.org/10.7124/bc.000089.
[8] A.C. Tripathi, S.J. Gupta, G.N. Fatima, K. Sonar, A. Verma, S.K. Saraf, 4-Thiazolidinones: the advances continue…, Eur. J. Med. Chem. 72 (2014) 52–77, https://doi.org/10.1016/j.ejmech.2013.11.017.
[9] J. Senkiv, N. Finiuk, D. Kaminskyy, D. Havrylyuk, M. Wojtyra, I. Kril, R. Stoyka, R. Lesyk, 5-Ene-4-thiazolidinones induce apoptosis in mammalian leukemia cells, Eur. J. Med. Chem. 117 (2016) 33–46, https://doi.org/10.1016/j.ejmech.2016.03.089.
[10] M.Z. Hernandes, M.M. Rabello, A.C.L. Leite, M.V.O. Cardoso, D.R.M. Moreira, D.J. Brondani, C.A. Simone, L.C. Reis, M.A. Souza, V.R.A. Pereira, R.S. Ferreira, J.H. McKerrow, Studies toward the structural optimization of novel thiazolylhydrazone-based potent antitrypanosomal agents, Bioorg. Med. Chem. 18 (22) (2010) 7826–7835, https://doi.org/10.1016/j.bmc.2010.09.056.
[11] E.B. da Silva, D.A.O.E. Silva, A.R. Oliveira, C.H. da Silva Mendes, T.A.R. dos Santos, A.C. da Silva, M.C.A. de Castro, R.S. Ferreira, D.R.M. Modeira, M.V.O. Cardoso, C.A. de Simone, V.R.A. Pereira, A.C. Lima Leite, Desing and synthesis of potent anti-Trypanosoma cruzi agents new thiazoles derivatives which induce apoptotic parasite death, Eur. J. Med. Chem. 130 (2017) 39–50, https://doi.org/10.1016/j.ejmech.2017.02.026.
[12] D.R.M. Moreira, A.C. Lima Leite, M.V.O. Cardoso, R.M. Srivastava, M.Z. Hernandes, M.M. Rabello, L.F. da Cruz, R.S. Ferreira, C.A. de Simone, C.S. Meira, E.T. Guimaraes, A.C. da Silva, T.A.R. dos Santos, V.R.A. Pereira, M.B.P. Soares, Structural design, synthesis and structure-activity relationships of thiazolidinones with enhanced anti-trypanosoma cruzi activity, ChemMedChem 9 (1) (2014) 177–188, https://doi.org/10.1002/cmdc.201300354.
[13] D. Steverding, X. Wang, Trypanocidal activity of the proteasome inhibitor and anticancer drug bortezomib, Parasit. Vectors. 2 (1) (2009) 29, https://doi.org/10.1186/1756-3305-2-29.
[14] A. Deterding, F. Dungey, K. Thompson, D. Steverding, Anti-trypanosomal activities of DNA topoisomerase inhibitors, Acta Trop. 93 (3) (2005) 311–316, https://doi.org/10.1016/j.actatropica.2005.01.005.
[15] C.A. Stein, R.V. LaRocca, R. Thomas, N. AcAtee, C.E. Myers, Suramin: an anticancer drug with a unique mechanism of action, J. Clin. Oncol. 7 (4) (1989) 499–508, https://doi.org/10.1200/JCO.1989.7.4.499.
[16] F.L. Meyskens, E.W. Gerner, Development of difluoromethylornithine (DFMO) as a chemoprevention agent, Clin. Cancer Res. 5 (5) (1999) 945–951 http://clincancerres.aacrjournals.org/content/5/5/945.
[17] S.M. Gomha, T.A. Salah, A.O. Abdelhamid, Synthesis, characterization, and pharmacological evaluation of some novel thiadiazoles and thiazoles incorporating

pyrazole moiety as anticancer agents, Monatsh. Chem. 146 (2015) 149–158, https://doi.org/10.1007/s00706-014-1303-9.
[18] S. Gomha, K. Khalil, H. Abdel-aziz, M. Abdalla, Synthesis and anti-hypertensive α-blocking activity evaluation of thiazole derivatives bearing pyrazole moiety, Heterocycles 91 (9) (2015) 1763–1773, https://doi.org/10.3987/COM-15-13290.
[19] S.M. Gomha, M.M. Edrees, F.M.A. Altalbawy, Synthesis and characterization of some new bis-pyrazolyl-thiazoles incorporating the thiophene moiety as potent anti-tumor agents, Int. J. Mol. Sci. 17 (2016) 1499, https://doi.org/10.3390/ijms17091499.
[20] A. Kryshchyshyn, D. Kaminskyy, P. Grellier, R. Lesyk, Trends in research of anti-trypanosomal agents among synthetic heterocycles, Eur. J. Med. Chem. 85 (2014) 51–64, https://doi.org/10.1016/j.ejmech.2014.07.092.
[21] T.K. Smith, B.L. Young, H. Denton, D.L. Hughes, G.K. Wagner, First small molecular inhibitors of *T. brucei* dolicholphosphate mannose synthase (DPMS), a validated drug target in African sleeping sickness, Bioorg. Med. Chem. Lett. 19 (2009) 1749–1752, https://doi.org/10.1016/j.bmcl.2009.01.083.
[22] D. Havrylyuk, B. Zimenkovsky, O. Vasylenko, C.W. Day, D.F. Smee, P. Grellier, R. Lesyk, Synthesis and biological activity evaluation of 5-pyrazoline substituted 4-thiazolidinones, Eur. J. Med. Chem. 66 (2013) 228–237, https://doi.org/10.1016/j.ejmech.2013.05.044.
[23] D. Havrylyuk, B. Zimenkovsky, O. Karpenko, P. Grellier, R. Lesyk, Synthesis of pyrazoline–thiazolidinone hybrids with trypanocidal activity, Eur. J. Med. Chem. 85 (2014) 245–254, https://doi.org/10.1016/j.ejmech.2014.07.103.
[24] J.B. Baell, Feeling nature's PAINS: natural products, natural product drugs, and pan assay interference compounds (PAINS), J. Nat. Prod. 79 (3) (2016) 616–628, https://doi.org/10.1021/acs.jnatprod.5b00947.
[25] A.R. Saltiel, J.M. Olefsky, Thiazolidinediones in the treatment of insulin resistance and type II diabetes, Diabetes 45 (12) (1996) 1661–1669.
[26] J. Ohkanda, F.S. Buckner, J.W. Lockman, K. Yokoyama, D. Carrico, R. Eastman, K. de Luca-Fradley, W. Davies, S.L. Croft, W.C. Van Voorhis, M.H. Gelb, S.M. Sebti, A.D. Hamilton, Design and synthesis of peptidomimetic protein farnesyltransferase inhibitors as anti-Trypanosoma brucei agents, J. Med. Chem. 47 (2) (2004) 432–445, https://doi.org/10.1021/jm030236o.
[27] R. Ettari, L. Tamborini, I.C. Angelo, N. Micale, A. Pinto, C. De Micheli, P. Conti, Inhibition of rhodesain as a novel therapeutic modality for human African trypanosomiasis, J. Med. Chem. 56 (14) (2013) 5637–5658, https://doi.org/10.1021/jm301424d.
[28] C.P. Lo, W.J. Croxall, 5-Alkoxymethylenerhodanines and their reactions with rhodanines, J. Am. Chem. Soc. 76 (1954) 4166–4169, https://doi.org/10.1021/ja01645a033.
[29] D. Atamanyuk, B. Zimenkovsky, V. Atamanyuk, R. Lesyk, 5-Ethoxymethylidene-4-thioxo-2-thiazolidinone as versatile building block for novel biorelevant small molecules with thiopyrano[2,3-*d*][1,3]thiazole core, Syn. Commun. 44 (2) (2014) 237–244, https://doi.org/10.1080/00397911.2013.800552.
[30] C. Xing, L. Wang, X. Tang, Y.Y. Sham, Development of selective inhibitors for anti-apoptotic Bcl-2 proteins from BHI-1, Bioorg. Med. Chem. 15 (5) (2007) 7826–7835, https://doi.org/10.1016/j.bmc.2006.12.020.
[31] V.A. Chebanov, S.M. Desenko, T.W. Gurley, Azaheterocycles Based on α,β-Unsaturated Carbonyls, Springer, 2008, 212 p.
[32] G.O. Derkach, S.M. Golota, Ya.O. Trufin, O.M. Roman, G.M. Sementsiv, I.L. Demchuk, I.I. Soronovych, R.V. Kutsyk, P. Grellier, R.B. Lesyk, Synthesis and biological activity of 5-aminomethylene-2-thioxotiazolidin-4-ones derivatives, Pharm. Rev. 2 (2017) 5–11 (in Ukrainian).
[33] Y. Bansal, O. Silakari, Multifunctional compounds: smart molecules for multifactorial diseases, Eur. J. Med. Chem. 76 (2014) 31–42, https://doi.org/10.1016/j.ejmech.2014.01.060.
[34] A. Kryshchyshyn, D. Kaminskyy, I. Netegayev, P. Grellier, R. Lesyk, Isothiochromenothiazoles – a class of fused thiazolidinone derivatives with established anticancer activity that inhibits growth of *Trypanosoma brucei brucei*, Sci. Pharm. 86 (2018) 47, https://doi.org/10.3390/scipharm86040047.
[35] A.P. Kryshchyshyn, D.V. Atamanyuk, D.V. Kaminskyy, P. Grellier, R.B. Lesyk, Investigation of anticancer and anti-parasitic activity of thiopyrano[2,3-d]thiazoles bearing norbornane moiety, Biopolym. Cell. 33 (3) (2017) 183–205, https://doi.org/10.7124/bc.00094F.
[36] A. Monks, D. Scudiero, P. Skehan, R. Shoemaker, K. Paull, D. Vistica, C. Hose, J. Langley, P. Cronise, A. Vaigro-Wolff, M. Gray-Goodrich, H. Campbell, J. Mayo, M. Boyd, Feasibility of a high-flux anticancer drug screen using a diverse panel of cultured human tumor cell lines, J. Nat. Cancer Inst. 83 (11) (1991) 757–766, https://doi.org/10.1093/jnci/83.11.757.
[37] M.R. Boyd, K.D. Paull, Some practical considerations and applications of the national cancer institute in vitro anticancer drug discovery screen, Drug Dev. Res. 34 (1995) 91–109, https://doi.org/10.1002/ddr.430340203.
[38] M.R. Boyd, in: B.A Teicher (Ed.), Cancer Drug Discovery and Development, Humana Press 2 (1997) 23–43.
[39] R.H. Shoemaker, The NCI60 human tumour cell line anticancer drug screen, Nat. Rev./Can. 6 (2006) 813–823, https://doi.org/10.1038/nrc1951.
[40] DTP Databases and Search Tools; 2018. < https://dtp.cancer.gov/databases_tools/data_search.htm > (accessed 1 November 2018).
[41] S.A.F. Rostom, Synthesis and in vitro antitumor evaluation of some indeno[1,2-c] pyrazol(in)es substituted with sulfonamide, sulfonylurea(-thiourea) pharmacophores, and some derived thiazole ring systems, Bioorg. Med. Chem. 14 (2006) 6475–6485, https://doi.org/10.1016/j.bmc.2006.06.020.
[42] L.J. Farrugia, WinGX and ORTEP for windows: an update, J. Appl. Cryst. 45 (2012) 849–854, https://doi.org/10.1107/S0021889812029111.
[43] O.V. Dolomanov, L.J. Bourhis, R.J. Gildea, J.A.K. Howard, H. Puschmann, OLEX2: a complete structure solution, refinement and analysis program, J. Appl. Cryst. 42 (2009) 339–341, https://doi.org/10.1107/S0021889808042726.
[44] A.L. Spek, Structure validation in chemical crystallography, Acta Cryst. 65 (2009) 148–155, https://doi.org/10.1107/S090744490804362X.
[45] CrysAlis PRO, version 1.171.39.46; Rigaku Oxford Diffraction: Yarnton, U.K.; 2018.
[46] G.M. Sheldrick, SHELXT – integrated space-group and crystal-structure determination, Acta Cryst. A 71 (2015) 3–8, https://doi.org/10.1107/S2053273314026370.
[47] G.M. Sheldrick, Crystal structure refinement with SHELXL, Acta Cryst. Sect. C Struct. Chem. 71 (2015) 3–8, https://doi.org/10.1107/S2053229614024218.
[48] CrysAlis PRO, version 1.171.37.35; Rigaku Oxford Diffraction: Yarnton, U.K.; 2014.
[49] I. Bastos, F. Motta, S. Charneau, J. Santana, L. Dubost, K. Augustyns, P. Grellier, Prolyl oligopeptidase of Trypanosoma brucei hydrolyzes native collagen, peptide hormones and is active in the plasma of infected mice, Microbes Infect. 12 (2010) 457–466, https://doi.org/10.1016/j.micinf.2010.02.007.
[50] S. Lethu, D. Bosc, E. Mouray, P. Grellier, J. Dubois, New protein farnesyltransferase inhibitors in the 3-arylthiophene 2-carboxylic acid series: diversification of the aryl moiety by solid-phase synthesis, J. Enzyme Inhib. Med. Chem. 1 (2013) 163–171, https://doi.org/10.3109/14756366.2011.643302.
[51] S. Al-Nasiry, N. Geusens, M. Hassens, C. Luyten, R. Pijnenborg, The use of AlamarBlue assay for quantitative analysis of viability, migration and invasion of choriocarcinoma cells, Hum. Reprod. 22 (5) (2006) 1304–1309, https://doi.org/10.1093/humrep/dem011.